AD NUMBER

AD819032

NEW LIMITATION CHANGE

TO

Approved for public release, distribution unlimited

FROM

Distribution authorized to U.S. Gov't. agencies and their contractors; Critical Technology; JUN 1967. Other requests shall be referred to Naval Postgraduate School, Monterey, CA.

AUTHORITY

USNPS ltr, 1 Oct 1971

UNITED STATES
NAVAL POSTGRADUATE SCHOOL

THESIS

AN EXPERIMENTAL INVESTIGATION OF SURFACE EFFECTS ON NUCLEATE POOL BOILING OF LIQUID NITROGEN FROM A HORIZONTAL SURFACE

by

Harold Wayne George

AN EXPERIMENTAL INVESTIGATION OF SURFACE EFFECTS ON NUCLEATE POOL BOILING OF LIQUID NITROGEN FROM A HORIZONTAL SURFACE

by

Harold Wayne George
Lieutenant, United States Navy
B. S., University of New Mexico, 1962

Submitted in partial fulfillment of the requirements for the degree of

MASTER OF SCIENCE IN MECHANICAL ENGINEERING

from the

NAVAL POSTGRADUATE SCHOOL
June 1967

Signature of Author Harold W. George

Approved by Paul J. Marto
Thesis Advisor

R. E. Newton
Chairman, Department of Mechanical Engineering

R. F. Rinehart
Academic Dean

ABSTRACT

The effect of various surface conditions on the characteristic boiling curve for liquid nitrogen was experimentally investigated. A circular horizontal flat plate five square centimeters in area was utilized as a boiler surface.

The surfaces investigated included mirror finished surfaces, etched surfaces, and surfaces with .0043 inch diameter artificial cylindrical cavities. Each of these surface conditions was used with Electrical Tough Pitch Copper and Nickel 200 boiling surfaces.

The results indicate that surface conditions significantly affect the heat transfer coefficients during nucleate pool boiling of liquid nitrogen. Results from hysteresis data indicate that once boiling sites become active they tend to remain active and produce higher heat transfer rates.

TABLE OF CONTENTS

LIST OF TABLES

LIST OF FIGURES

TABLE OF SYMBOLS AND ABBREVIATIONS

A	Area of heater surface exposed to liquid nitrogen (cm^2)
d	differential
h_{fg}	Latent heat of vaporization $\frac{\text{calories}}{\text{gm}}$
H	Immersion depth of boiler surface in fluid (cm)
k_w	Thermal conductivity of wall (watts/cm ^oK)
k_l	Thermal conductivity of liquid (watts/cm ^oK)
K_i	Constant
P_b	Barometric Pressure (mm Hg.)
P_c	Barometric Pressure correction for temperature (mm Hg.)
P_o	Standard Pressure (760 mm Hg)
Q/A	Heat flux per unit area in boiler wall (watts/cm^2)
R	Gas Constant $\frac{\text{calories}}{\text{gm } ^oK}$
r	cavity radius (cm)
T_o	Saturation temperature at standard pressure (^oK)
T_s	Saturation temperature at liquid pressure (^oK)
T_w	Temperature at the boiler wall surface (^oK)
ΔT	$(T_w - T_s)$ Temperature difference between the boiler surface (^oK) and fluid saturation temperature at liquid pressure
W	Power (watts)
x	Distance of thermocouple from boiler surface (cm)
γ	Specific weight (dynes/cm^3)
ρ_v	Density of vapor (gm/cm^3)
σ	Surface Tension (dynes/cm)

SECTION 1

INTRODUCTION

Background

The role of cryogenic fluids in industry and the space program is becoming ever more important. Cryogenic fluids have many possible uses. Sittig (12) discusses a few of these uses. Preservation of blood and vital organs by the Medical Profession is accomplished using cryogenic fluids. Cryogenic Electronics (or Cryotronics) uses liquified gases to improve performance of masers, lasers, infra-red detectors and many other complicated systems. New methods of metal fabrication rely heavily on cryogenic fluids. The expanding use of cryogenic liquids has made it necessary to explore in more detail the mechanisms of cryogenic boiling heat transfer. Since liquid nitrogen is readily available through liquification and fractionization of air, it was chosen as the best and cheapest liquified gas for use in the present investigation. It is the purpose of this investigation to study cryogenic boiling heat transfer during nucleate boiling and how it is affected by varying surface conditions.

Previous Research

Cryogenic heat transfer by nucleate boiling is a relatively new field. The forerunner of the current investigation, Maynard (3) investigated nucleate boiling using a variety of surfaces with liquid nitrogen. He related the effects of contaminants and roughness on the characteristic boiling curve. Almgren and Smith (6) investigated

the inception of nucleate boiling and the parameters which affect the phenomenon of patchwise boiling. They determined that the spreading of a boiling patch was a function of the density of potential nucleating sites, i.e., the surface condition of the boiler surface. Bewilogua, Knoner, and Wolf (16) investigated heat transfer in boiling hydrogen, neon, nitrogen, and argon using an electrically heated capillary as the boiler. Lyon (15) investigated pool boiling heat transfer coefficients and peak nucleate boiling fluxes for liquid nitrogen, liquid oxygen, and mixtures of the two. His experiments, using gold, copper and several chemical films, determined the effect of roughness on pool boiling heat transfer. Seader, Miller, and Kalvinskas (14) conducted an extensive survey of available information on heat transfer to boiling hydrogen, nitrogen and oxygen. They have summarized boiling theory, experimental data and important physical properties on the three cryogenic fluids for use as a reference.

Whereas cryogenic heat transfer is a relatively new field, nucleate boiling of non-cryogenic fluids has been investigated in great detail. Young and Hummel (9) and many others have studied the effect of surface conditions using water as a working fluid. Berenson (11) used n-pentane and carbon tetrachloride with surfaces of copper, nickel, and inconel for investigation of surface effects. Marto and Rohsenow (8) used liquid sodium and investigated the surface effects for a great variety of boiling surfaces ranging from mirror finishes to porous plates.

Objective

The primary objective of this research was to investigate the effects various surface conditions have on the nucleate boiling phase of the characteristic boiling curve, using existing equipment where feasible. A secondary objective was to re-design the existing boiler to remove the problem of rogue nucleation sites encountered by Maynard (3), and to provide for a quick-open quick-close boiler seal for use in changing surfaces.

SECTION 2

DESCRIPTION OF EQUIPMENT

The bulk of the equipment used in this investigation was designed by and manufactured for Maynard (3). Only the boiler diaphragm, boiler enclosure and boiler vacuum seal were designed by the author.

Boiler Test Section

1. Heaters

Use was made of existing heaters used by Lt. M. D. Maynard. The heaters were fashioned from 19 inch long inconel sheathed (.045 inches diameter) Nichrome wire heating elements manufactured by the American Standard Company. Insulation material between the sheath and the wires was magnesium oxide. These heating wires were wound by hand into a flat disc shaped coil of approximately one inch in diameter.

Since the nucleate boiling portion of the characteristic boiling curve was to be investigated, Figure 12, a maximum heat flux of approximately 20 watts/cm^2 was needed. This value of heat flux required a maximum voltage across the heater of 65 volts, with a maximum current of 1.55 amps.

A sheathed heater was selected to insure maximum reduction of electrical noise in the vicinity of the test surface and to provide a surface which could be used with a silver solder braze.

2. Transition Section

The transition sections, Figure 13, were machined out of Electrical Tough Pitch Copper bar stock. The sections were .993

inches in diameter and .315 inches in length. These sections served the purpose of smoothing out any discontinuities of heat flux from the heater.

3. Stainless Steel Disc

These discs, Figure 13, used only with the copper boilers, provided a thermal resistance to insure that the heaters would be at approximately the same temperature as when used with the nickel specimens. These one inch diameter discs were punched from .025 inches thick stainless steel 321 sheet stock.

4. Boiler plates

The boiler plates were cylindrical in shape and machined to the dimensions shown in Figure 11. The length of each cylinder was selected to give a temperature gradient large enough to determine heat flux density with an error of less than 10 per cent at maximum heat flux. In each boiler four .035 inch diameter holes were drilled at uniform distances from the boiling surface and at intervals of 90° from each other Figure 11. These .480 inch deep holes were drilled in the specimen to accommodate thermocouples.

5. Boiler Diaphragm

The boiler diaphragm, used to support the boiler in the enclosure, was made from Nickel 200 to the dimensions shown in Figure 7. This configuration was selected so that the boiler plates and diaphragms could be removed from the assembly with relative ease. The semi-circular ring on the diaphragm is the upper half of the boiler vacuum seal. The section of the diaphragm near the boiler was machined to

a thickness of .023 inches to insure that the heat loss due to thermal conduction horizontally out of the boiler test section would be kept at a minimum. Nickel 200 was selected because of its low thermal conductivity and its ability to be electroplated and soldered more readily than stainless steel. Stainless steel is stronger and has a lower thermal conductivity but experiments by Korbelak and Okress (1) have determined that electroplating is accomplished only by a very difficult and involved process.

6. Boiler enclosure

The enclosure, consisting of two pieces, was machined from stainless steel circular bar stock to the dimensions shown in Figure 7. The can has a wall thickness of .035 inches throughout its length except at the upper end where the thickness increases to .200 inches to accommodate the lower half of the boiler vacuum seal. The center section of the bottom plate fits snugly into the can and is silver soldered in place to provide a good vacuum seal.

7. Boiler Vacuum Seal

The seal configuration was selected to provide a good vacuum seal without becoming too complex or too difficult to machine. The upper half of the seal has a .10 inch diameter semicircular cross section, Figure 8, with an overall diameter of 1.670 inches. The lower half is a circular 'Vee' groove, diameter 1.670 inches, with an included angle of 90°. The groove is .050 inches deep and .100 inches wide at the top, Figure 8. When the diaphragm and can are placed together the semi-circular ring fits into the 'Vee' groove and

makes contact on both sides providing a double seal. An annular ring of .016 inches thick Teflon is placed between the two seating surfaces and the assembly is pulled together using eight 3/16 inch steel studs. Teflon was chosen as the seal material because of its low coefficient of thermal expansion, and its plastic nature. The low coefficient of thermal expansion insures that the sealing material will not shrink away from the seats at liquid nitrogen temperatures. The plastic nature is necessary to insure that the Teflon will flow under load into any scratches or imperfections on the two seating surfaces.

Vacuum Systems

Two vacuum systems were required for this investigation. A medium vacuum system (10^{-6} mm Hg.) was used for thermal insulation of the test boiler and the inner dewar. A low vacuum (10^{-3} mm Hg.) was used for environmental control of the boiler fluid. Both are shown schematically in Figure 10.

1. Thermal Insulation System

A large capacity Welch Duo-Seal 1402 B two stage mechanical pump served as roughing pump for the system and as a fore pump for the diffusion pump. The rated capacity of the roughing pump was 140 liters/min. of free air displacement with an ultimate vacuum of 10^{-4} mm Hg. A Consolidated Vacuum Corporation MCF 300 Fractionating Diffusion pump with a rated capacity of 290 liters/min. provided the medium vacuum required. The ultimate vacuum of the diffusion pump was 2×10^{-7} mm Hg. Dow-Corning 705 Silicon Oil was used

in the diffusion pump because of its resistance to oxidation and very low backstreaming characteristics.

The diffusion pump was equipped with a thermal cutout switch and a diaphragm vacuum microswitch. These switches were installed to protect the diffusion pump in the event of losing fore pump vacuum or overheating. A liquid nitrogen cold trap was placed between the diffusion pump and the test unit to capture condensable vapors and reduce backstreaming. The cold trap was connected to the valve manifold by a 1 1/2 inch O.D. x .035 inch wall thickness stainless steel pipe. From the valve manifold, .500 inch x .035 inch wall stainless steel tubing leads to the inner dewar and to the boiler through flexible couplings.

Stainless steel tubing was used whenever possible to reduce the problem of outgassing within the system. Viton "A" O rings were used at all flanges because of their low outgassing characteristics.

2. Environmental Control Vacuum

A National Research Corporation type 2S mechanical pump, rated at 33 liters/min. was used for environmental control. The ultimate vacuum of this pump was 3×10^{-3} mm Hg. The main purpose of this pump was to outgas the test surface and dewar to reduce the possibility of contamination of the liquid nitrogen.

Dewars

The 3.1 inch inner dewar (shown schematically in Figure 10) held the working fluid and the test surface. An O-ring was placed between the dewar and the top flange in order that the pressure over the fluid

could be controlled. The dewar thermal shield vacuum was connected to the valve manifold through the flexible coupling using a Pyrex-Kovar Housekeeping seal. A permanent vacuum was not used because the system was designed for future use with liquid helium which penetrates warm glass. The vacuum in a permanently sealed dewar would eventually be lost. A dewar with permanent vacuum would be quite acceptable for systems using only liquid nitrogen.

The outer dewar (I.D. 4.7 inches) was manufactured with a sealed permanent vacuum of 10^{-6} mm Hg. This dewar when filled with liquid nitrogen provides a radiation and thermal barrier for the inner dewar. The dewars were made with double silvered radiation shields and an off-set, aligned, unsilvered, vertical strip, .8 inches wide. The unsilvered strip allowed visual observation of the test surface.

Instrumentation

1. Temperature Sensing

ISA type T copper-constantan grounded junction thermocouples sheathed with stainless steel 304 were selected. The sheath had an O.D. of .0325 inches with a wire diameter of .007 inches. Copper-constantan was selected over iron-constantan thermocouples because a greater degree of accuracy could be attained. Each of the thermocouples was calibrated using methods described in appendix A.

After calibration, four thermocouples were inserted into the .035 inch holes in the boiler plate. Apiezon 'N' vacuum grease was used in the holes to facilitate assembly and to provide good thermal contact.

The thermocouple leads were fed through the vacuum support tube, through a Conax MHC Multiple-hole packing gland (ceramic followers with a Teflon sealant), and then attached to a 24 position rotary switch. Liquid nitrogen was used as the reference with care being taken to insure stratification did not occur. A fifth thermocouple was located in the boiling liquid nitrogen approximately one inch above the test surface. The function of this thermocouple was to detect changes in the bulk temperature of the liquid nitrogen during operation.

The rotary switch and the thermocouple junctions were located inside a shielded zone box (fabricated from 5/8 inch plywood and lined with aluminum foil). This shielding prevented any undesirable Seebeck emfs from being generated. The thermocouple output was amplified by a Hewlett Packard Differential Amplifier model 8875 and fed to a Hewlett Packard automated D.C. digital voltmeter, model 405C. The signals had an amplification factor of 1000 which was necessary in order to obtain three significant figures from the microvolt output of the thermocouples. The minimum sensitivity of the voltmeter without amplification was one millivolt. The output of the digital voltmeter was recorded on a Hewlett Packard digital recorder.

2. Pressure Sensing

Two low vacuum National Research Corporation, Mode 734 matched thermocouple gages were used to monitor the pressure in the system. Minimum readable pressure was 5×10^{-3} mm Hg. One of the thermocouple gages measured the pressure at the roughing pump inlet while the other measured the pressure at the diffusion

pump inlet. At higher vacuum a National Research Corporation type 724 cold cathode ionization gage with a 524 sensing head was used. Pressures down to 10^{-7} mm Hg. could be measured using the gage. The cold cathode ionization gage was located at the valve manifold in order to measure boiler pressure as accurately as possible.

SECTION 3

EXPERIMENTAL PROCEDURES

Preparation of Test Surfaces

In order to define the microstructure of the test specimens for future correlation the methods of preparing each test surface are described in detail.

A machined boiler test surface was brazed to the nickel diaphragm and the heater was soldered to the copper transition section using silver solder (M.P. 1170°F.). Upon cooling, the two sections of the total assembly were soldered together using Eutecrod 157 solder (M.P. 425°F.) with the stainless steel disc inserted between the two partial assemblies (copper specimens only). The lower melting point solder was used for the bonding of the two partial assemblies to allow for changing of heaters if necessary. The total assembly was then placed in a lathe and a small 'Vee" groove cut in the nickel diaphragm at the periphery of the test surface. The 'Vee' groove was then filled with silver solder. The purpose of this 'Vee' groove was to allow the silver solder to flow into the small annular slot between the diaphragm and the boiler. This was done in order to alleviate the problem of premature nucleate boiling from the interface. The specimen was then cleaned to remove all flux and other contaminants on the assembly.

1. Mirror Finish Nickel

The boiler surface and diaphragm was sanded by pressing against a rotating dry 320 grit carborundum belt. The sample was then

rotated 90° and sanded by hand over dry 0 emery paper, rotated 90° again and sanded over dry 3/0 emery paper. The samples were stroked only long enough to remove the scratches from the preceding process. The samples were then wet polished on four 8 inch Buehler metallurgical polishing wheels. Wheel one was covered with canvas. By rotating 90° from the direction of sanding on the 3/0 emery paper and using a 500 grit carborundum and water suspension as an abrasive, all previous scratches were removed. The specimen was then cleaned using a soapy water solution to remove all traces of the 500 grit carborundum. The sample was again rotated 90° and placed on the second wheel which was covered with Kitten ear (a felt like material) with 7 micron alumina as the abrasive. Upon completion of polishing on the second wheel the sample was again cleaned with the soap solution and then flushed with methanol and dried under a hot air jet. The sample was then placed on a third wheel covered with a fine velvet imbedded with 3 micron diamond dust. Methanol was used on this wheel as the wetting agent. The sample was manually rotated opposite to the direction of rotation of the polishing wheel to insure that the polishing was not done in only one direction. The specimen was again cleaned using the soap solution and the methanol. The final wheel was also covered with a very smooth velvet and imbedded with one micron diamond dust using methanol as the wetting agent. After completion of polishing on the final wheel the sample had a very bright mirror finish with no visible scratches. A photomicrograph was then taken of the boiler diaphragm interface to check for complete bonding

of the silver solder and elimination of the rogue nucleation sites. It was observed that the bonding had been accomplished and the rogue sites did not exist. Figure 1 shows a typical interface.

2. Mirror Finish Copper

The copper specimens were polished in the same manner as the nickel specimen. Whereas in the nickel specimen no rogue sites occurred, in the copper specimen rogue sites were present in the form of small holes in the silver solder. The holes occurred because the copper retained heat longer than the diaphragm and bubbles resulted. In order to eliminate these bubble holes the copper specimens were then electroplated after the final polishing. The electroplating was accomplished using procedures outlined by Carlson (2). A solution containing 24 oz./gal. of copper sulfate ($CuSO_4 \cdot 5H_2O$) and 6 oz./gal. of sulfuric acid was prepared. A pure copper plate cut to the same approximate size as the boiler plate was used as the anode with the plating surface as the cathode. For the size boiler surface to be plated, it was calculated that a cathode current density of 35 amp/ft^2 (when the cathode and anode were separated by a distance of two inches) would yield the best plate. Using this current density, approximately 30 minutes was required to plate the surface. After plating, the surface was again polished using the four metallurgical polishing wheels as before. After polishing, the surface had the appearance of a solid piece of copper, with the rogue sites being eliminated. Since Maynard's (3) results for an oxidized surface show that oxidation at 200-230°F. had almost no effect on the boiling curve,

care was not taken to prevent oxidation at room temperature. The specimen was however wrapped in lens paper to prevent scratching and contamination by other means.

3. Nickel Etched

A clean, mirror finished nickel surface (as outlined above) was etched with a solution of 50 per cent acetic acid and 50 per cent nitric acid for period of approximately 30 seconds. The whole surface was etched including the silver solder interface. However, upon operation of this surface, boiling started from this interface rather than from the boiler proper, so the specimen was repolished and the interface covered with grease. After the etching process had been completed and the specimen cleaned to remove the grease, the interface was observed to be in the same condition as a freshly polished specimen. A photomicrograph was then taken to determine the microstructure of the surface. Figure 4. Upon rerunning the surface it was found that the grease coat on the interface during etching had eliminated this premature nucleate boiling.

4. Copper Etched

A clean, mirror finished, plated copper specimen was etched with a solution of potassium dichromate for a period of approximately three minutes. A photomicrograph was then taken to determine the microstructure. Figure 3.

5. Artificial Cylindrical Cavities

A clean, mirror finished specimen was placed in a lathe and a .0043 inch diameter cylindrical cavity, Figure 2, was drilled in

the center of the boiling surface using a sphinx pivot drill manufactured by Levin, Inc. The depth of the cavity was estimated to be approximately .015 inches. The specimen was then again repolished on the four wheels and the hole cleaned by manually rotating a drill in the cavity.

Testing Procedures

The two heater leads were soldered to the power wires, checked for continuity, and then separately wrapped with Teflon tape to reduce the possibility of shorting upon installation. Prior to insertion of the thermocouples into their respective holes, the holes were filled with Apiezon 'N' grease. The grease insures that good thermal contact will be maintained while testing the specimen. The boiler test section was then placed into the can and a check was made to insure that the Teflon sealant ring was in place between the two halves of the boiler seal. Prior to tightening the eight studs used to apply the sealing force to the seal, the heater was again checked for continuity. The heater studs were then torqued down to 35 inch pounds using five inch pound increments so that no warpage of the seal would occur.

After rechecking for heater continuity, the boiler insulating vacuum valve was opened allowing the boiler to be placed under the vacuum of the roughing pump only. While the pump down of the boiler was taking place the inner dewar was cleaned with water and ethanol and hung in place. Upon connection to the vacuum system through the quick-disconnect seal, the inner dewar vacuum valve was opened and evacuation begun. The environmental control vacuum system

vent was then closed and pumpdown begun on the inside of the inner dewar. The purpose of evacuating the inner dewar working area was to insure that all water vapor and other airborne contaminants would be removed.

When the pressure in the boiler reached approximately 25 microns the diffusion pump was started and its cold trap filled with liquid nitrogen. Approximately 40-45 minutes was required for the pump down of the thermal system. During this waiting period the amplifier-voltmeter combination was turned on and allowed to warm up. The outer dewar was then cleaned and hung in place.

When the thermal system reached approximately 10^{-5} mm Hg., a small amount of liquid nitrogen was introduced into the outer dewar. Sufficient time was allowed for the outer dewar to cool before it was slowly filled to within one inch of the top. A cotton cloth was then placed in the annular space between the two dewars to retard contamination with water vapor in the air.

The inner dewar was then vented and liquid nitrogen was introduced at a very slow flow rate. The flow rate was low enough to insure that the system would not receive a thermal shock but high enough to insure that a steady stream of gaseous nitrogen emerged from the dewar from the filling port. The exhausting of gaseous nitrogen continuously was necessary so that air would not backstream into the dewar and contaminate the liquid nitrogen with water vapor and other impurities in the air. Once the liquid nitrogen level was above the boiling surface, the filling rate was increased and the dewar filled to approx-

imat ely 40 cm. above the boiler surface. Upon completion of filling, a Plexiglas view port was placed over the filling port. The reference thermocouple dewar was then filled to a depth of 10 cm. and covered. By this time, due to the action of the cryopumping in the boiler can and dewar, the pressure had dropped to approximately 4×10^{-6} mm Hg. The system was now ready for a data run.

Atmospheric temperature and pressure, liquid nitrogen height in the dewar and boiler pressure were recorded prior to commencement of a run.

A data run consisted of applying power to the heater at approximately five watt intervals to a maximum of 50 watts and at 10 watt intervals when reducing power. After each increase in power the emf readings displayed visually on the digital voltmeter were recorded along with heater voltage and amperage. At various times through the run the digital voltmeter was checked against a Rubicon potentiometer. Approximately 1.5-2.0 minutes were required between increases in power for equilibrium to be established. Equilibrium was assumed to be reached when the output emfs of the thermocouples were steady and did not vary with time. On several of the runs, multiple cycles (increases to maximum power, decrease to zero) were made in order to determine hysteresis effects. Between cycles the boiler was allowed to cool only long enough to deactivate all sites.

The system was shut down by de-energizing the heater, venting the boiler and removing both dewars. The roughing pump preceding the diffusion pump was left in operation between runs to outgas the

system up through and including the valve manifold. When the test surface had warmed to room temperature, the boiler was disassembled and a micrometer reading taken to determine the true distance from the boiling surface to the first thermocouple.

SECTION 4

RESULTS AND DISCUSSION

Investigation was limited to a total of seven surfaces. In an effort to reproduce results, two of the surfaces (mirror copper) were identical. Heat fluxes as high as 24.5 watts/cm^2 and ΔT's as high as 19.8°K. were attained without complications.

Results

Mirror Copper Surfaces

Two mirror copper surfaces were evaluated and the results plotted as Figure 14. In each case upon increasing heat flux, heat transfer was by free convection alone. This free convection heat transfer continued until a wall superheat of approximately 10°K., and an associated heat flux (Q/A) of 4.5-5.0 watts/cm^2 was reached. At this point the entire surface began nucleating. The surfaces were not being observed at the exact instant of inception so the location of the first nucleation site is unknown. With the inception of nucleation a decrease in $T_w - T_s$ occurred. The ΔT decreased from the maximum to approximately 5.5°K. The heat flux associated with the new ΔT was approximately 5.5 watts/cm^2. The data for the two surfaces is plotted as Figure 14 with Maynard's (3) results included for comparison.

Mirror Nickel Surface

The mirror nickel specimen behaved in a manner similar to the mirror copper specimens, Figure 16, in that the free convection portion of the curve was followed by a large drop in ΔT at the inception

of nucleation. As before, the entire surface began nucleating. The values of wall superheat and heat flux at inception were different as would be expected. The maximum ΔT achieved was 19.8°K. with a corresponding Q/A of approximately 3.5 watts/cm^2.

Copper Etched

The etched copper specimen, Figure 15, again behaved as did the mirror finished specimens. However, the decrease in ΔT associated with the inception of boiling was much less severe and occurred at a lower ΔT. During nucleate boiling a much higher Q/A results, for a given ΔT than resulted for the mirror finished specimens, therefore a higher heat transfer coefficient is obtained.

Nickel Etched

The etched nickel specimen, Figure 16, was the only surface investigated which did not exhibit the same characteristics as the previous cases. At the lowest heat flux, boiling occurred from several isolated sites. Full nucleation occurred when the heat flux reached 1.85 watts/cm^2 and the ΔT reached 3.3°K.

Artificial Cylindrical Cavity Nickel

This specimen again exhibited the initial free convection, followed by the decrease in ΔT at inception, Figure 16. The drop occurred at a ΔT of approximately 10.5°K. and a corresponding heat flux of 1.7 watts/cm^2. Start of nucleation was observed for this surface. The first bubble emerged from the artificial cavity and was followed by a rapid spreading of nucleation sites radially outward from the cavity. Upon decreasing power to the heater it was observed that

the artificial cavity was the last active site on the specimen.

Cylindrical Cavity Copper

This surface behaved in the same manner, Figure 15, as the cylindrical cavity nickel surface. The maximum heat flux reached before inception was approximately 4.8 watts/cm^2 at a ΔT of 7.8°K. It was observed on this specimen that upon reducing heater power to the point where only the artificial cavity and one other site were nucleating, that the artificial cavity appeared to be boiling more rapidly and with a larger bubble size. When power was again increased (after all sites except the artificial cavity had been deactivated) the curve was displaced to the right of the original curve obtained while decreasing power input.

TABLE I

SUMMARY OF NUCLEATE BOILING DATA

Surface Condition	Flux at Inception watts/cm^2	ΔT at Inception $^\circ$K.	Resulting Drop in ΔT $^\circ$K.	Last Observed active site on decreasing flux watts/cm^2	ΔT at last observed site $^\circ$K.
Mirror Cu #1	3.9	8.4	2.8	*	*
Mirror Cu #2	4.7	9.6	4.3	4.1	0.6
Mirror Ni	3.4	19.8	9.8	1.4	6.2
Etched Cu	5.8	4.7	1.1	4.3	0.1
Etched Ni	0.48	0.6	**	%	%
Cyl Cav Cu	4.7	7.8	1.5	4.4	0.53
Cyl Cav Ni	1.8	10.5	2.7	1.1	1.8

*No data taken on decreasing flux
**Etched Nickel did not exhibit the decrease in ΔT
%Last data point taken while many sites still active.

TABLE II

SUMMARY OF HEAT TRANSFER COEFFICIENTS

Surface condition	BTU/Hr. Ft.^{2} $^\circ$F Last data point prior to inception	Following Inception	At max. heat flux
Mirror Copper #1	830	2480	4860
Mirror Copper #2	905	1830	4410
Mirror Nickel	304	742	1565
Etched Copper	2170	3410	5290
Etched Nickel	(a)	1034 (b)	4750
Cylindrical Cavity Cu.	1100	1680	4460
Cylindrical Cavity Ni.	302	537	2145

(a) Boiling occurred at the lowest heat flux investigated. Only a few sites were active at start.

(b) Full surface nucleation

Discussion

The results indicate that for each surface (except etched nickel) a large drop in wall superheat occurred at inception of nucleation. For each surface there was a marked increase in the heat transfer coefficient h_b associated with inception of nucleate boiling. The increases ranged from a three fold increase (830 to 2480 BTU/Hr. Ft^2 $^oF.$) for the mirror copper surface to an increase of approximately 78 per cent (302 to 537 BTU/Hr. Ft^2 $^oF.$) for the mirror finished nickel specimen with the artificial cavity. These higher heat transfer coefficients at inception are due to the formation and growth of vapor bubbles at nucleation sites.

As the heat flux was increased after inception, the heat transfer coefficient likewise increased. This increase of h_b is due to the increasing density of active nucleating sites. At progressively higher heat fluxes more and more cavities on the surface are activated due to overspreading of inactive sites by bubbles from neighboring active sites.

Effect of Etching

For both the copper and the nickel specimens, etching had the effect of greatly increasing the heat transfer coefficient at all points on the boiling curve. The etched copper specimen had a h_b at inception of 3410 BTU/Hr. Ft^2 $^oF.$ compared to approximately 2000 BTU/Hr. Ft^2 $^oF.$ for the mirror finished specimen. The nickel specimen also had a higher h_b for the etched surface than for the mirror finished surface. This difference in h_b becomes very apparent at maximum

heat flux where the etched nickel specimen had a h_b of 4750 BTU/Hr. $Ft.^2\ ^oF.$ while the mirror finished nickel specimen had a h_b of only 1365 BTU/Hr. $Ft.^2\ ^oF.$

Upon comparing the heat transfer coefficients for the two etched specimens at the points where full surface nucleation occurred, it can be seen that etching had a greater effect on the nickel specimen. By etching, the smooth surface is replaced by a very uneven granular surface. This granular surface is a result of the orientation of grains in the materials. Because the etchant more readily attacks the grain boundaries than the grains themselves, many potential nucleating sites are created. Upon inspection of the photomicrographs of the two etched surfaces, it is seen that the grains are much larger in the nickel specimen. Because the grains are larger, the etched out grain boundaries are larger resulting in larger cavities for potential nucleation sites.

Griffith and Wallis (17) have determined theoretically that the temperature difference $(T_w - T_s)$ necessary to cause a bubble to grow in a cavity is a function of the cavity mouth radius. The larger the cavity, the smaller the ΔT required for boiling to occur. Since the cavity size for the nickel specimen is larger, nucleation will occur sooner.

Effect of Artificial Cavities

The addition of an artificial cavity to a mirror finished surface has two major effects. First nucleation occurs at a lower ΔT and second a higher rate of heat transfer is obtained.

The first observed active site was the artificial cavity, indicating that entrapped vapor was present to some extent in the cavity. Bankoff (13) has concluded analytically that inception of boiling can only occur at surface cavities containing a liquid-vapor interface. Other cavities, microscopic in nature are inherent to the surface and are assumed to contain entrapped vapor to a smaller degree. Since the artificial cavity is by far the largest cavity available as a potential nucleation site it is the first to become active.

The observed behavior of the surface upon nucleation of the cavity indicates that one active site tends to activate other sites. This is apparent from the fact that the whole surface was covered with active sites once the artificial cavity became active.

Equations representing the criterion for incipient boiling from an artificial cavity were used (See Appendix C) to determine how well experimental results agreed with theory. These equations state that boiling can occur i.e. a bubble will grow only if the liquid temperature at a distance y = r(cavity mouth radius) from the wall is greater than the critical vapor temperature. These equations when modified can be used to determine the critical wall temperature in terms of heat flux, saturation temperature, and critical vapor temperature necessary to produce incipient boiling. The theoretically determined wall temperature for the nickel specimen with the .0043 inches diameter cylindrical cavity was 84.9°K. The experimentally determined T_w was 87.95°K. Examination of the photomicrograph of this cavity revealed that the cavity mouth was not circular but somewhat egg shaped. Since

the theoretical equations are derived for a cavity with a circular mouth exact correlation could not be obtained.

Effect of Material

The use of copper results in better heat transfer for all surface conditions except for the etched surfaces (See effect of etching). This improved heat transfer rate is due to the higher bubble generation rate resulting from the higher thermal diffusivity of the copper. These results agree with Maynard's (3) results and with Berenson's (11) results for n-pentane.

Hysteresis Effects

A considerable amount of hysteresis was observed upon reduction of power to the heater. Figures 17, 18, and 19 illustrate this. Upon initial nucleation of the surface, only a small number of the potential active sites were boiling. As heat flux was increased, more of these sites became active. Once active, they tended to remain active. Because the active sites had the tendency to remain active, upon decreasing heater power, higher rates of heat transfer were obtained. Data for the mirror copper specimen indicates that a drop in wall superheat of approximately two degrees occurred without an appreciable drop in heat flux. This decrease of two degrees results in an increase in the heat transfer coefficient of approximately 500 BTU/Hr. Ft.^{2} $^\circ$F.

SECTION 5

CONCLUSIONS WITH RECOMMENDATIONS

The results discussed lead to the following conclusions:

1. The surface condition of the boiler has a significant effect on the characteristic boiling curve for liquid nitrogen.

2. Etching results in an approximate increase of 45 per cent in the heat transfer rate for copper and an increase of approximately 170 per cent for nickel.

3. Addition of one artificial cavity (.0043 inches in diameter) in the boiling surface increases the heat transfer rate of mirror finished copper by 15 per cent and mirror finished nickel by 30 per cent.

4. Boiler material affects the boiling curve of liquid nitrogen.

The following recommendations are made for future investigations using cryogenic fluids:

1. Continue studies with many cylindrical cavities.

2. Study the effect of reentrant and other geometry artificial cavities.

3. Use liquid neon and liquid helium to further increase the knowledge of cryogenic boiling heat transfer.

4. Investigate other types of material and their effects on the boiling curve of liquid nitrogen.

ACKNOWLEDGMENT

The author wishes to express his gratitude for the assistance and the beneficial suggestions given him by Professor Paul J. Marto. He also wishes to thank Mr. J. Beck and Mr. K. Smith for their assistance on this project. Special thanks are due Mr. Kenneth Mothersell for extra time and effort spent working on this project.

LIST OF REFERENCES

1. Korelak, A., and Okress, E., "Plating of stainless steel and other alloys containing Chromium, Nickel, and Cobalt." Material from Engineering Department of Westinghouse Electric Co.

2. Carlson, A. F., "Acid Copper Plating", Metal Finishing Guidebook, pp. 324-328.

3. Maynard, M. D., "An experimental Investigation of the effect of Surface Conditions on Nucleate Pool Boiling Heat Transfer to Liquid Nitrogen from a Horizontal Surface" USNPGS Thesis, USNPGS, Monterey, California.

4. Powell, R. L. and Sparks, L. L., "Available Low Temperature Thermocouple Information and Services", NBS report 8750, Feb. (1965).

5. Hodgman, C. D., "Handbook of Chemistry and Physics", Cleveland, Ohio, Chemical Rubber Company.

6. Almgren, D. W. and Smith, J. L., Jr., "The inception of Nucleate Boiling with Liquid Nitrogen", Cryogenic Engineering Laboratory, MIT, Contract No. AF19(628)-4972, Project No. 8608.

7. Barron, R., "Cryogenic Systems", McGraw Hill Inc. (1965).

8. Marto, P. J. and Rohsenow, W. M., "The effect of Surface Conditions on Nucleate Pool Boiling Heat Transfer to Sodium", D. Sci. Thesis, MIT(1965) (AEC Code: Report MIT-3357-1).

9. Young, R. K. and Hummel, R. L., "Improved Nucleate Boiling Heat Transfer", Chemical Engineering Progress, 60 p. 53, July (1964).

10. Johnson, V. J. (Ed.), "A compendium of the properties of Materials at Low Temperature", Phase II, December (1961).

11. Berenson, P. J., "Experiments on Pool Boiling Heat Transfer" Int'l Journal of Heat and Mass Transfer, 5, October (1962).

12. Sittig, M. (Ed.), "Cryogenics", Research and Applications, D. VanNostrand Co., Princeton, New Jersey (1963).

13. Bankoff, S. G., "Ebullition from Solid Surfaces in the Absence of a Pre-existing Gaseous Phase" Trans. ASME May (1957), Journal of Heat Transfer, 79, page 735 (1957).

14. Seader, J. D., Miller, W. S., and Kalvinskas, L. A., "Boiling Heat Transfer for cryogenics" Rocketdyne R-5598, May (1964).

15. Lyon, D. N., "Peak Nucleate-Boiling Heat Fluxes and Nucleate Boiling Heat Transfer Coefficients for Liquid Nitrogen, Liquid oxygen, and their mixtures in Pool Boiling at atmospheric Pressure," Int'l Journal of Heat and Mass Transfer, Vol. 7, pp. 1097-1116, Pergamon Press (1964).

16. Bewilogua, L., Knoner, R., and Wolf, G., "Heat Transfer in Boiling Hydrogen, Neon, Nitrogen and Argon", Lehrstuhl fur Physik tiefer Temperaturen der Technischen Universitat Dresden, Germany, Cryogenics, Vol. 6 No. 1 February (1966).

17. Griffith, P., and Wallis, D. W., "The Role of Surface Conditions in Nucleate Boiling", ASME-A. I. Ch. E. Heat Transfer Conference, Storrs, Conn. (1959).

APPENDIX A

Calibration of Thermocouples

Direct instrument calibration against secondary standards was chosen as the best means to achieve the high degree of accuracy required. The amplifier-voltmeter combination was calibrated at the scene of the experiment in order to zero correct the output for electronic noise present in the lab. A standard cell of 1.01944 volts was used in combination with a voltage divider to generate a small signal (0-600 microvolts). The amplifier was first zero adjusted using a shorting wire between the input leads. The amplifier was then adjusted so that the digital voltmeter agreed with the output measured by a Rubicon potentiometer known to be accurate to within $\pm$ 5 microvolts.

Calibration of the thermocouples was accomplished using two known boiling points. In each case the reference was liquid nitrogen. Technical grade oxygen (99.5 per cent purity) and technical grade methane (99.5 per cent purity) were used as the calibrating points. Each thermocouple was immersed in liquid nitrogen and a zero reading recorded. The thermocouple was then placed in the liquid oxygen and the liquid methane and emfs for these fluids were recorded. Generated emfs for both liquids remained constant over a period of more than two hours. Both calibrating liquids were liquified in the laboratory by the author. This was accomplished by passing gaseous oxygen and methane through a copper coil immersed in liquid nitrogen.

Each liquid's boiling point was corrected to standard pressure and with the recorded emfs became input to a computer program developed by NBS Cryogenic Laboratories at Boulder, Colorado (4). The program which was available at cost from NBS, compared the spot calibration with the NBS calibration table, calculated a correction factor and then generated a working table for temperatures from 0 to 300°K. A sample working table is given as appendix B.

Since each thermocouple produced virtually the same resultant emf, an average value for the eight thermocouples calibrated was used as the input to the computer program. Using an average value, an error of no more than 0.8 microvolts was introduced at the liquid oxygen reference point. At the liquid methane reference point, the maximum error introduced was 1.0 microvolts.

Table A-1

Thermocouple Calibration Summary

LN_2-LOX

Average 216.7 μv.

T.C. No.	Corrected LOX μv.	deviation from average μv.	difference °K.
1.	216.7	0.0	0.0
2.	216.3	0.4	0.023
3.	216.7	0.0	0.0
4.	217.2	0.5	0.028
5.	215.9	0.8	0.045
6.	217.1	0.4	0.023
7.	216.7	0.0	0.0
8.	217.0	0.3	0.017

The fourth digit of the generated emf for each thermocouple was determined by averaging the emfs generated over a one minute period with readings being taken every five seconds.

Table A-2

THERMOCOUPLE CALIBRATION SUMMARY

LN_2-LCH_4

average 597.7 μv.

T.C. No.	corrected LCH_4 μv.	deviation from average μv.	difference ^{o}K
1.	598.4	0.7	0.035
2.	598.2	0.5	0.025
3.	598.3	0.4	0.020
4.	596.7	1.0	0.049
5.	597.9	0.2	0.009
6.	597.6	0.1	0.005
7.	596.7	1.0	0.049
8.	597.0	0.7	0.035

Table A-3

COMPARISON OF LOX vs LCH_4 GENERATED WORKING TABLES

Temp. ^{o}K.	LOX μv.	LCH_4 μv.	Difference LOX-LCH_4 μv.	Difference ^{o}K.
80	42.9	42.1	0.8	0.049
85	126.0	124.1	1.9	0.112
90	212.5	209.7	2.8	0.160
95	302.1	298.3	3.8	0.206

Table A.-3 (Continued)

100	395.0	390.1	4.9	0.258
105	491.1	485.2	5.9	0.296
110	590.2	583.4	6.8	0.341

APPENDIX B

GENERATED THERMOCOUPLE WORKING TABLE

THERMOCOUPLE TABLE FOR COPPER VS CONST., ISA TYPE TP-TN, BASED ON NAT. BUR. OF STANDARDS PUB. R-188 WITH CALC. MULT. FACTOR OF .97621. LN^2-LOX CALIB. LOT NO. 1. USERS REFERENCE TEMPERATURE 77.340 DEG. K. TEST DATE 28 MAR 1967. BY H. W. GEORGE.

TEMP DEG K	EMF MIC V	DELEMF MIC V	DE/DT MIC V/DGK	TEMP DEG K	EMF MIC V	DELEMF MIC V	DE/DT MIC V/DGK
66	-172.6	14.4	14.452	91	230.1	17.6	17.744
67	-158.0	14.6	14.595	92	247.9	17.8	17.873
68	-143.4	14.6	14.737	93	265.9	18.0	18.002
69	-128.6	14.8	14.876	94	283.9	18.0	18.131
70	-113.7	14.9	15.014	95	302.1	18.2	18.260
71	-98.6	15.1	15.149	96	320.4	18.3	18.388
72	-83.3	15.3	15.281	97	338.9	18.5	18.516
73	-68.0	15.3	15.410	98	357.4	18.5	18.643
74	-52.6	15.4	15.539	99	376.2	18.8	18.770
75	-37.0	15.6	15.668	100	395.0	18.8	18.896
76	-21.2	15.8	15.797	101	413.9	18.9	19.022
77	-5.4	15.8	15.926	102	433.1	19.2	19.148
78	10.6	15.9	16.056	103	452.3	19.2	19.274
79	26.7	16.1	16.186	104	471.6	19.3	19.400
80	42.9	16.2	16.315	105	491.1	19.5	19.525
81	59.2	16.3	16.445	106	510.7	19.6	19.650
82	75.7	16.5	16.575	107	530.4	19.7	19.775
83	92.3	16.6	16.705	108	550.2	19.8	19.899
84	109.1	16.8	16.835	109	570.1	19.9	20.023
85	126.0	16.9	16.965	110	590.2	20.1	20.147

APPENDIX F (Continued)

86	143.0	17.0	17.094	111	610.5	20.3	20.271
87	160.1	17.1	17.224	112	630.8	20.3	20.395
88	177.4	17.3	17.354	113	651.3	20.5	20.519
89	194.9	17.5	17.484	114	671.9	20.6	20.643
90	212.5	17.6	17.614	115	692.6	20.7	20.766

APPENDIX C

SAMPLE CALCULATIONS WITH ERROR ANALYSIS

The following assumptions were used in data reduction.

1. Thermocouple working tables were accurate to $\pm$ 0.1 ^{o}K. from 77 to 85 ^{o}K., to $\pm$ 0.2 ^{o}K. from 85 to 100 ^{o}K. and to $\pm$ 0.3 ^{o}K. from 100 to 110 ^{o}K.

2. Liquid nitrogen used had a purity of 99.95 per cent and the same quality used for calibration.

3. Thermocouple hot junction position is known to $\pm$ 0.01 inches.

4. Barometric pressure was accurate to 0.1 mm Hg.

5. Thermal conductivities of materials agree to within five per cent of the reference curves, Figures 5 and 6.

6. Measured depths of nitrogen are accurate to within 1 cm.

Point 5 of the cylindrical cavity Nickel specimen was chosen for sample calculations.

Table C-1

REDUCED THERMOCOUPLE DATA

T. C.	Location from boiling surface inches	Corrected Temperature ^{o}K
1.	.383 $\pm$ .01	90.09 $\pm$ .2
2.	.308 $\pm$ .01	89.67 $\pm$ .2
3.	.233 $\pm$ .01	89.25 $\pm$ .2
4.	.158 $\pm$ .01	88.83 $\pm$ .2

Heat Flux

In order to determine heat flux, the temperature readings of the four thermocouples were plotted against distance from the boiling surface. In each case, a linear plot resulted and the slope of the line (dT/dx) was recorded.

Using the Fourier heat conduction equation and knowing the average thermal conductivity based on temperature distribution between thermocouples 1 and 4.

$$Q/A = k_w \frac{dT}{dx} \approx k_w \frac{\Delta T}{\Delta X} \qquad \text{C-1}$$

$$Q/A = \left(\frac{.765 \text{ watts}}{cm\,^\circ K}\right)\left(1.26\,^\circ K\right)\left(\frac{1}{.572 cm}\right) = 1.70 \ \frac{\text{watts}}{cm^2}$$

when error limits are included this becomes $1.70 \pm .18$ watts/cm^2.

In order to determine T_w Equation C-1 is rearranged to give

$$T_4 - T_w = \frac{Q}{A}\frac{X_4}{k_4} \qquad \text{C-2}$$

where subscript 4 refers to thermocouple number 4 position.

Upon substitution of the value of heat flux, equation C-2 yields

$$T_4 - T_w = 1.70\left(\frac{.401}{.762}\right) = .884\,^\circ K$$

Using a T_4 of 88.83 $^\circ$K, T_w = 87.95 $^\circ$K.

The most probable error for the wall temperature is

$$\Delta T_w = \sqrt{(\Delta T_4)^2 + (T_4 - T_w)^2\left[\left(\frac{\Delta Q/A}{Q/A}\right)^2 + \left(\frac{\Delta k}{k}\right)^2 + \left(\frac{\Delta X_4}{X_4}\right)^2\right]} \qquad \text{C-3}$$

$\frac{\Delta Q/A}{Q/A}$ Fractional error in heat flux = .1056

$\frac{\Delta k}{k}$ Fractional error in thermal conductivity = .0500

$\frac{\Delta X_4}{X_4}$ Fractional error in thermocouple 4 position = .0555

$\Delta T_1 = \pm .2°K$ from table C-1

Applying these factors to equation C-3 yields

$$\Delta T_w = \pm .231 °K.$$

Saturation Temperature, T_s

The depth of the liquid nitrogen above the boiler surface was recorded before and after the run. At the start the depth was 40 cm and at the end the depth was 32 cm. An average of 36 was used for determining static pressure head.

Upon changing units the standard pressure depth equation $P_{head} = \gamma H$ takes the form

$$P_{head} = \left(\frac{50.4\ lb}{ft^3}\right)\left(\frac{36 \pm 4\ cm}{2.54\ cm/in}\right)\left(\frac{ft^3}{1728\ in^3}\right)\left(\frac{760\ mm\ Hg}{14.71\ lb/in^2}\right)$$

$P_{head} = 21.30 \pm 2.37$ mm Hg.

$\Delta P_s = 760.0 - 770.5 \pm .1 = 10.5 \pm .1$ mm Hg.

P_c was determined by interpolation from reference 5 for barometric pressure and temperature.

$P_c = -2.63$ mm Hg.

$$\Delta P_{TOT} = P_{HEAD} + \Delta P_s + P_c \qquad \text{C-4}$$

$$= 21.30 + 10.5 - 2.63 = 29.17 \pm 3.37 \text{ mm Hg.}$$

To determine the change in saturation temperature T_s the perfect gas relationship was used to change the Clausius Clapeyron equation to the form $\Delta T_s = \frac{R T_o^2 \Delta P_{TOT}}{h_{fg} P_o}$

$$\Delta T_s = \left(\frac{.07088\ BTU}{lb\,°R}\right)\left(\frac{lb}{857\ BTU}\right)(77.34\,°K)^2\left(\frac{\Delta P_{TOT}\ mm\ Hg}{760\ mm\ Hg}\right)\left(\frac{9°R}{5°K}\right)$$

$$= .01167\ \Delta P_{TOT}\ °K$$

Substitution from equation C-4 for P_{total}

$$\Delta T_s = (.01167)(29.17) = .342 \pm .0395\ °K$$

$$T_s = T_o\,[REF\ (7)] + \Delta T_s\ °K \qquad C\text{-}5$$

$$T_s = 77.347 + (.342 \pm .0395) = 77.699 \pm .0395\ °K$$

$T_w - T_s$

Simple subtraction yields

$$\Delta T = T_w - T_s = (87.95 \pm .231) - (77.699 \pm .0395)$$

$$\Delta T = 10.25 \pm .27\ °K$$

APPENDIX D

CALCULATION OF T_w FOR INCIPIENCE OF NUCLEATE BOILING

In order to correlate experimental data with theory, use is made of the theoretical equations used by Marto and Rohsenow (8) for the incipience of nucleate boiling. Equations for critcal vapor temperature and liquid temperature are combined to yield the equation

$$T_W - \frac{Q}{A}\frac{r}{k_L} = \frac{T_{SAT}}{1 - \frac{2\sigma}{\rho_v h_{fg} r}} \qquad D\text{-}1$$

Since $\frac{2\sigma}{\rho_v h_{fg} r}$ = Constant (K_1)

$$T_w - \frac{Q}{A}\frac{r}{k_L} = \frac{T_{SAT}}{1-K_1} \quad OR \quad T_w = \frac{T_{SAT}}{1-K_1} + \frac{Q}{A}\frac{r}{k_L} \qquad D\text{-}2$$

Using values of ρ_v , k_L and h_{fg} from Barron (7) and r as determined from the photomicrograph of the mouth of the artificial cavity nickel surface.

$$K_1 = 2\left(\frac{8.48\ dynes}{cm}\right)\left(\frac{ft^3}{.288\ lb}\right)\left(\frac{lb}{85.7\ BTU}\right)\left(\frac{1}{.00734\ cm}\right)\left(\frac{BTU}{1.055\times10^{10}\ dyne\ cm}\right)\left(\frac{1728\ in^3}{ft^3}\right)\left(\frac{(2.54)^3\ cm^3}{in^3}\right)$$

$$K_1 = .252 \times 10^{-3}$$

and $1-K_1 = .999747 \approx 1.0$

$$\therefore\ T_w = T_{SAT} + \frac{Q}{A}\frac{r}{k_L} \qquad D\text{-}3$$

Using the experimentally determined heat flux at the last data point prior to inception of boiling and T_s of the liquid nitrogen as determined in appendix C.

$$T_w = 77.70 + \left(\frac{1.70 \text{ watts}}{\text{cm}}\right)\left(.00734 \text{ cm}\right)\left(\frac{m^\circ K}{.13655 \text{ watts}}\right)\left(\frac{100 \text{ cm}}{m}\right)$$

$$T_w = 86.90 \ ^\circ K$$

The experimentally determined value of T_w was 87.95°K. This represents an error of 1.2 per cent.

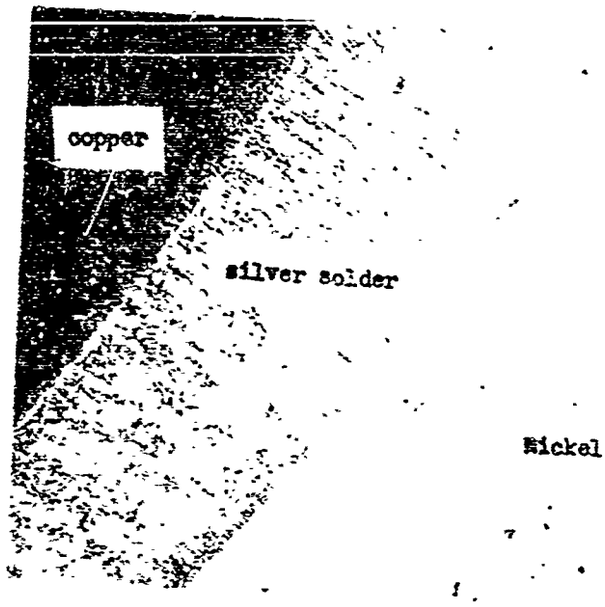

FIGURE 1. PHOTOMICROGRAPH OF COPPER-DIAMOND INTERFACE

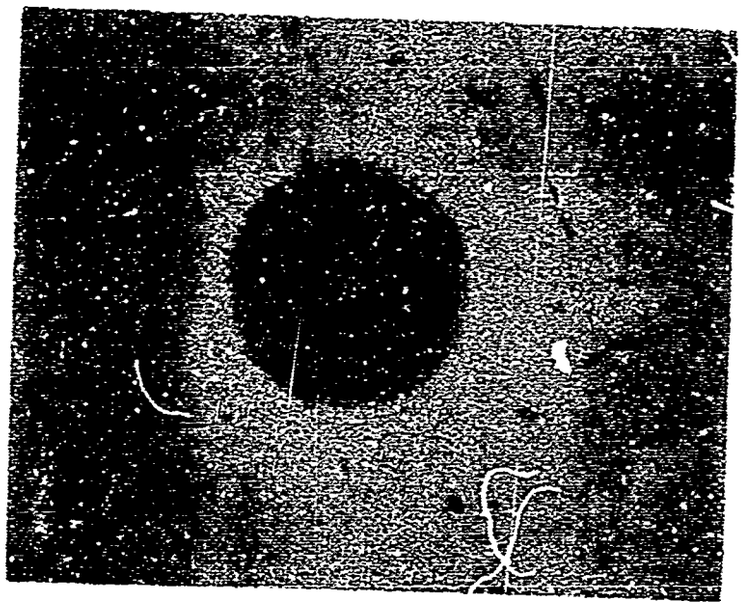

FIGURE 2. PHOTOMICROGRAPH OF [illegible]

FIGURE 3

FIGURE 4

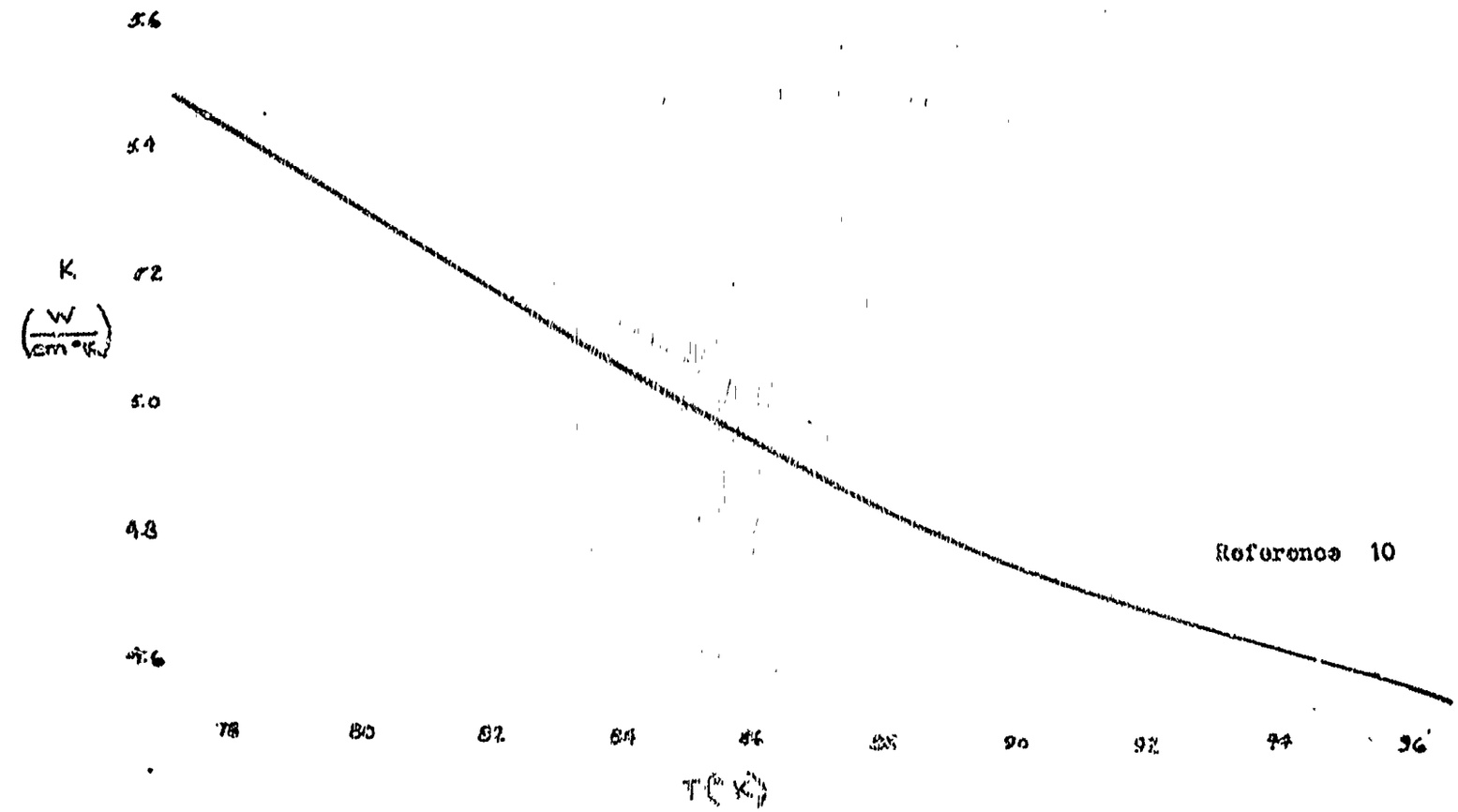

FIGURE 5 THERMAL CONDUCTIVITY OF COPPER USED IN TEST ELEMENT

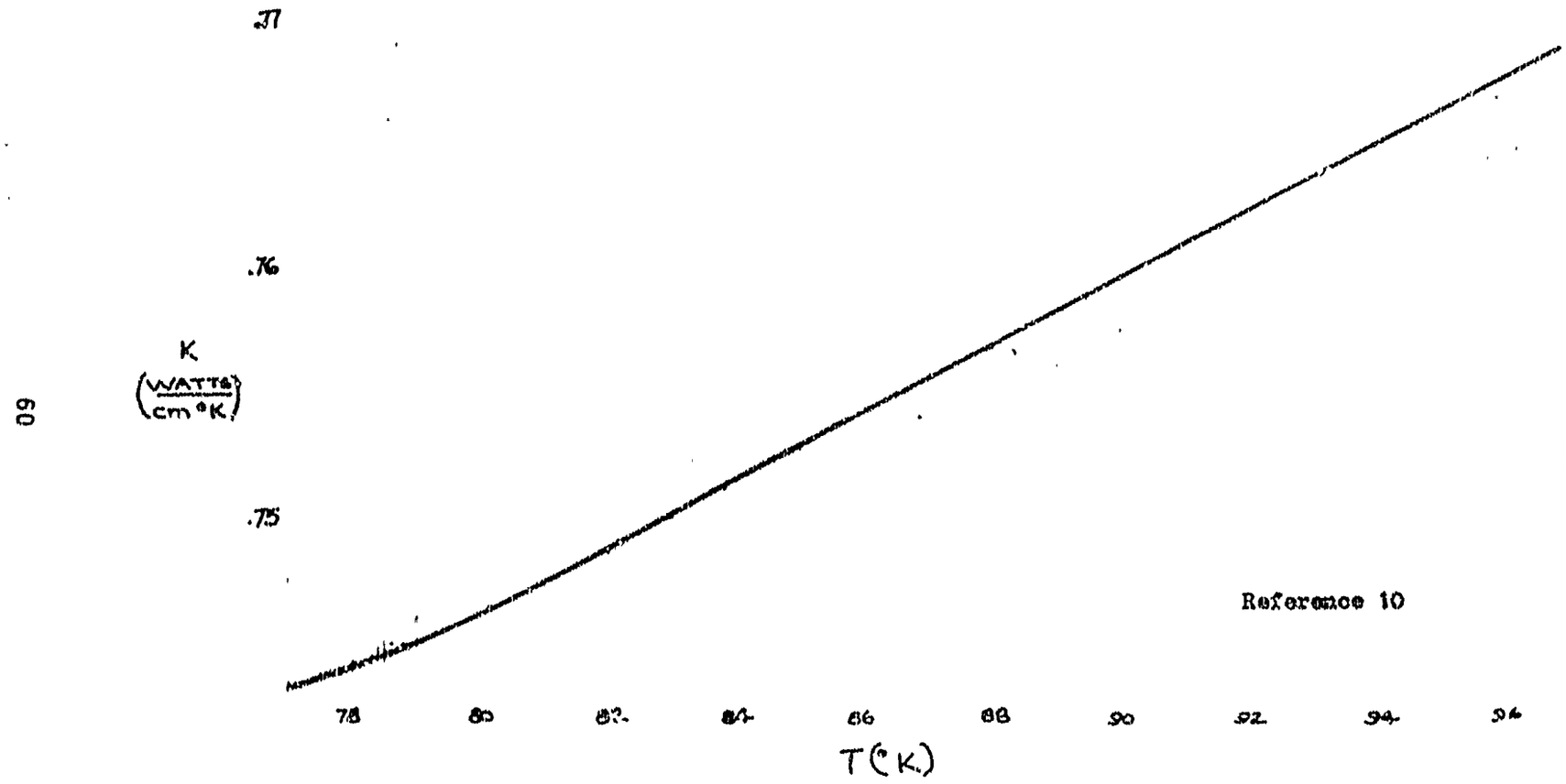

FIGURE 6 THERMAL CONDUCTIVITY OF NICKEL 200 USED IN TEST ELEMENT

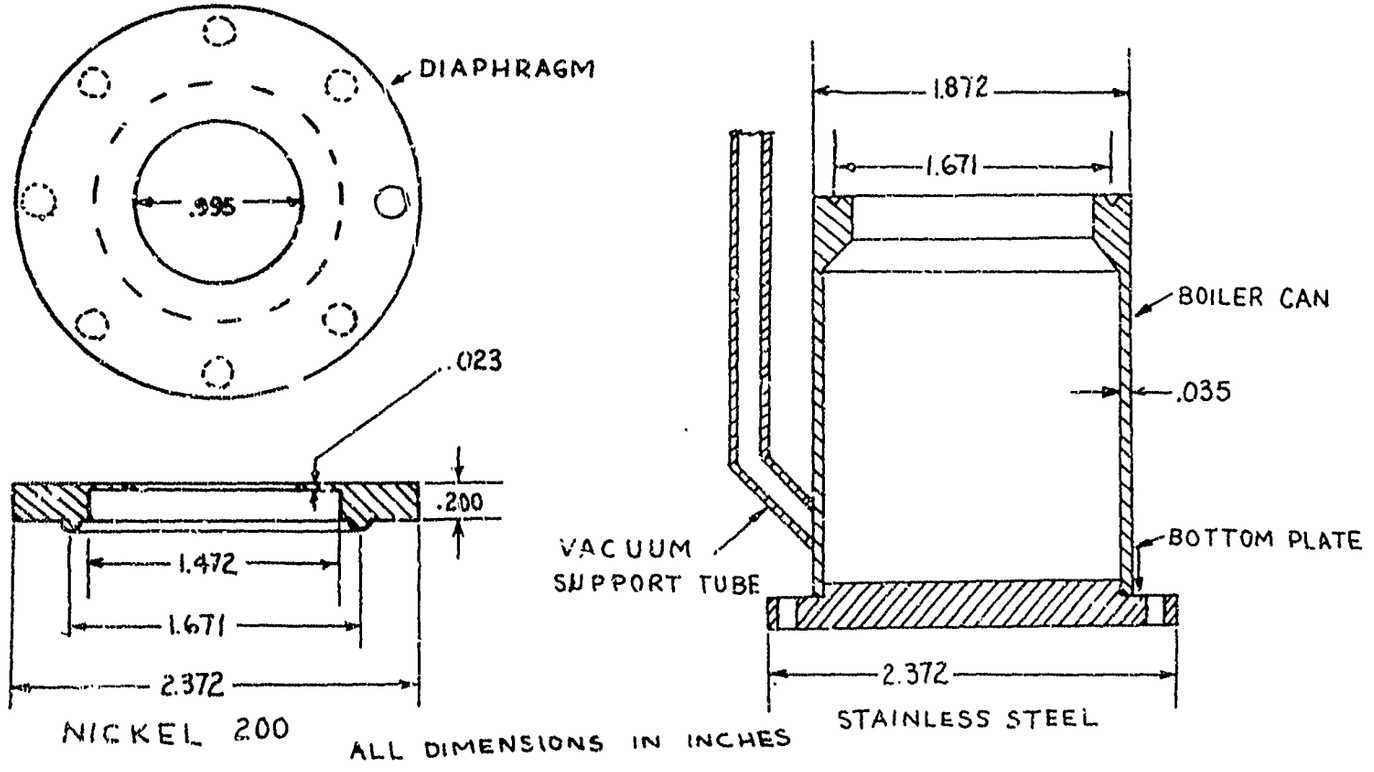

FIGURE 7 BOILER ASSEMBLY

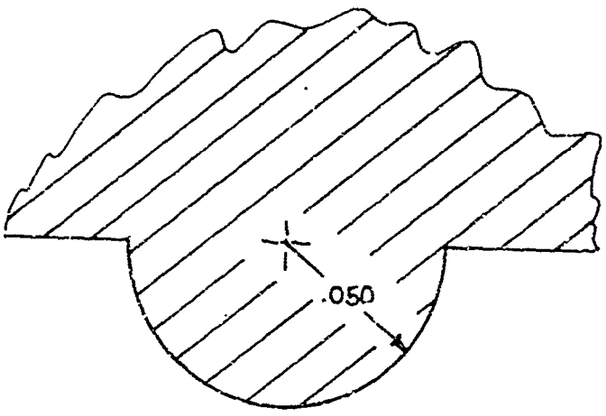

1 INCH = .050 INCHES

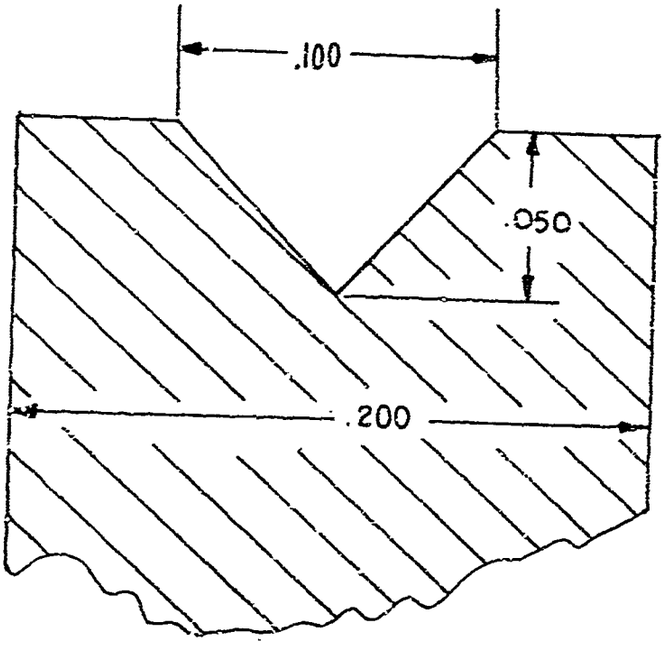

FIGURE 8 EXPANDED VIEW OF SEAL

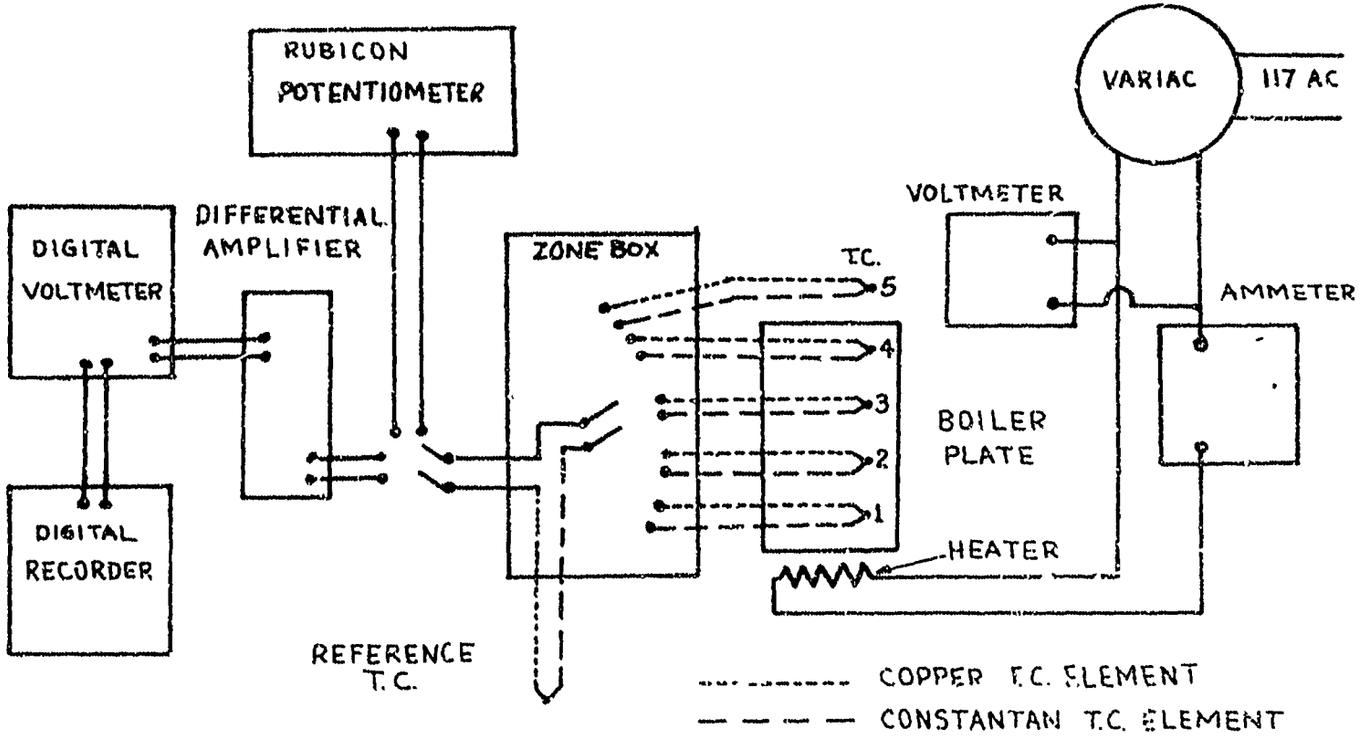

FIGURE 9 SCHEMATIC DIAGRAM OF HEATER & T.C. CIRCUITS

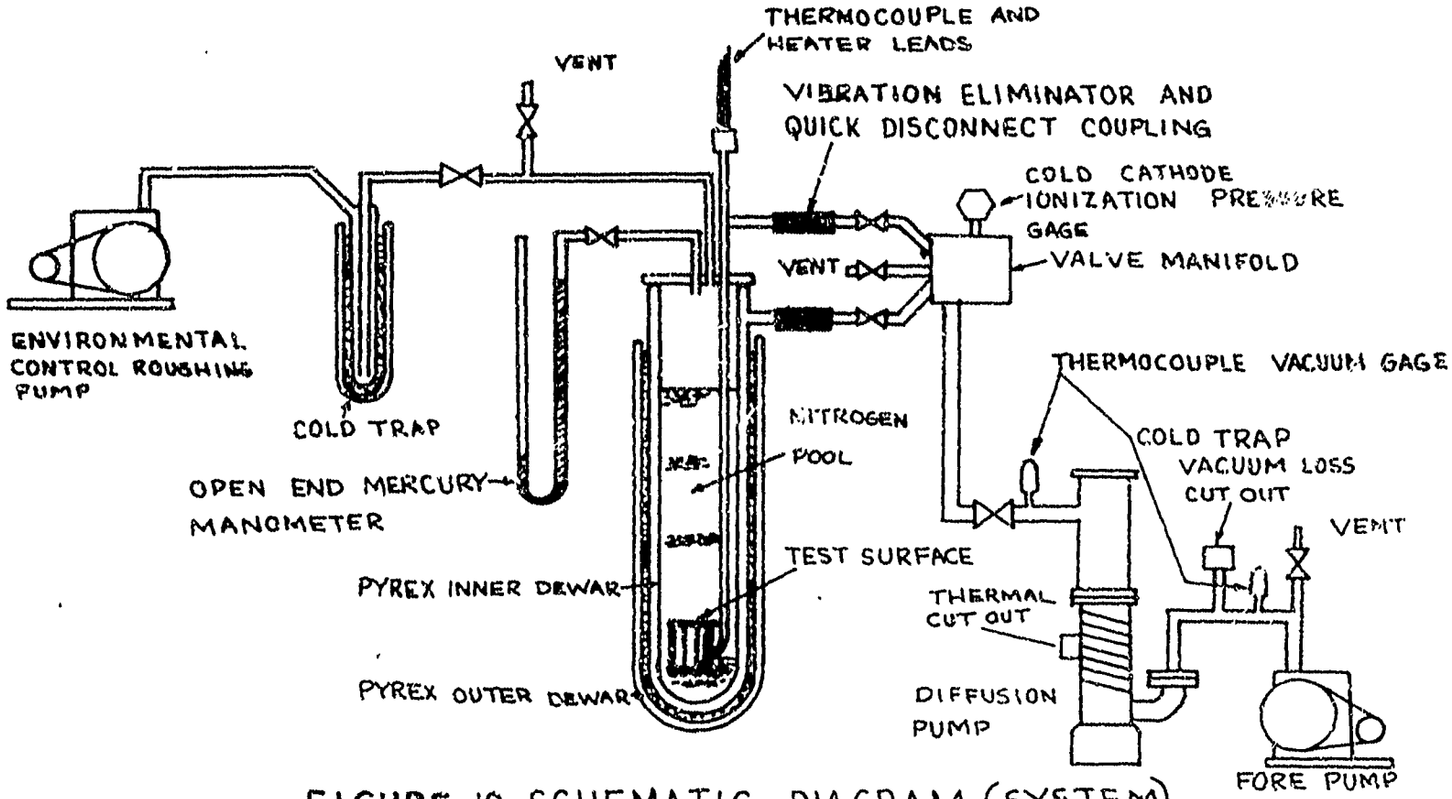

FIGURE 10 SCHEMATIC DIAGRAM (SYSTEM)

ELECTRICAL
TOUGH PITCH COPPER

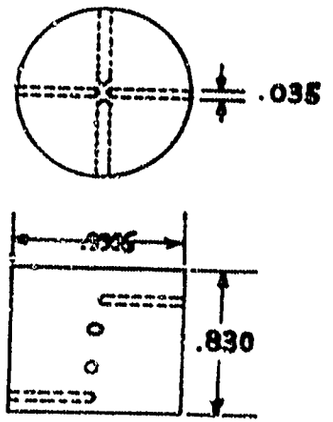

T.C.	℄ DISTANCE TO BOILER SURFACE
1.	.660
2.	.505
3.	.355
4.	.205

NICKEL 200

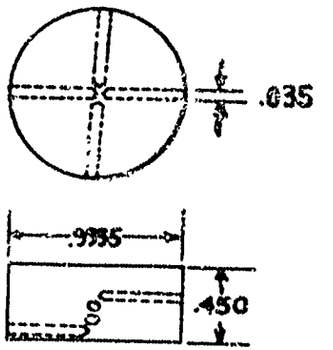

T.C.	℄ DISTANCE TO BOILER SURFACE
1.	.402
2.	.327
3.	.252
4.	.177

ALL DIMENSIONS IN INCHES

FIGURE 11 DETAIL OF BOILER

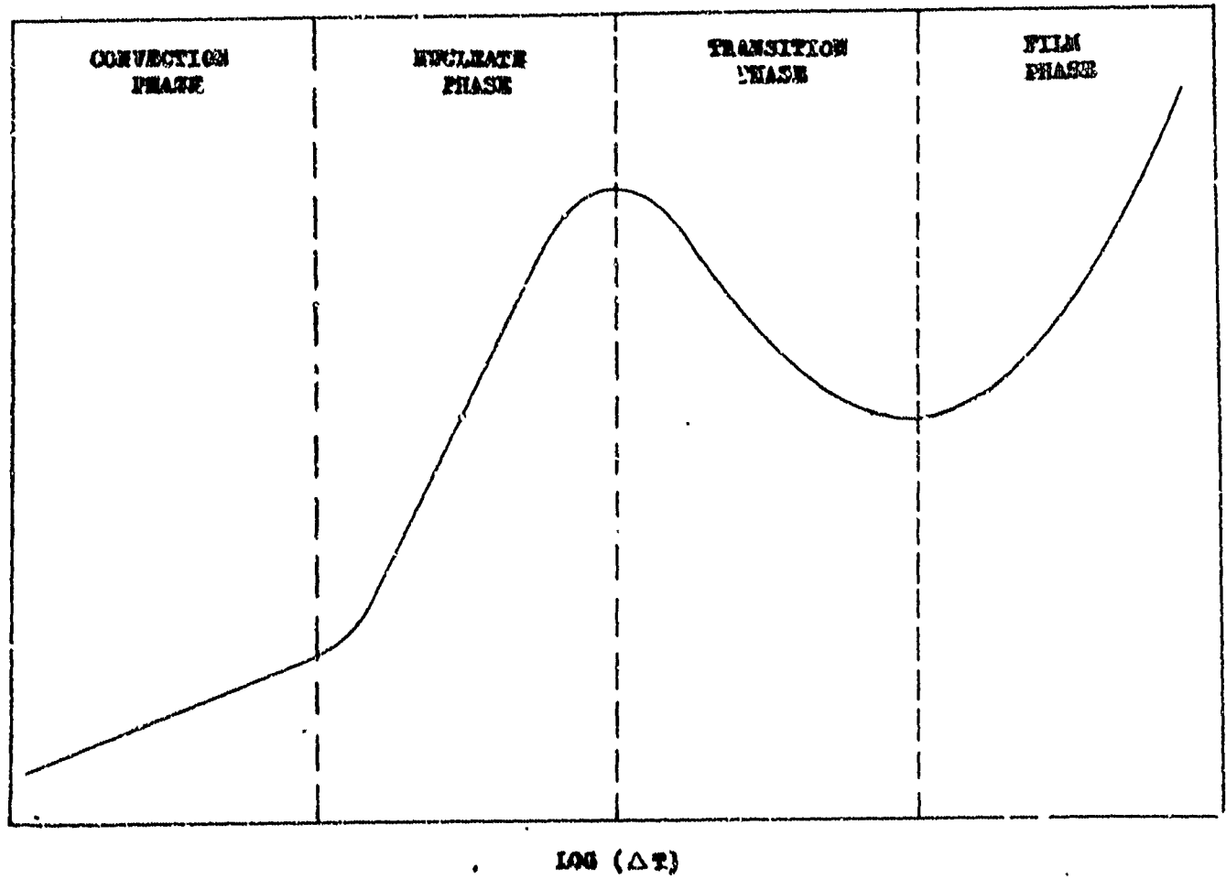

FIG. 12 CHARACTERISTIC BOILING CURVE

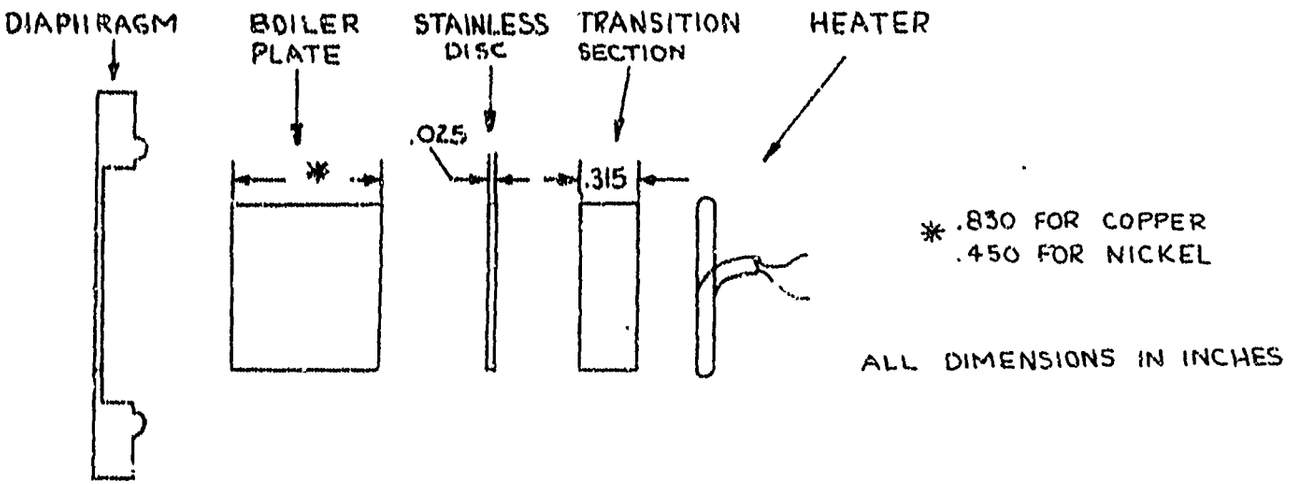

FIGURE 13 SCHEMATIC OF BOILER LAYOUT

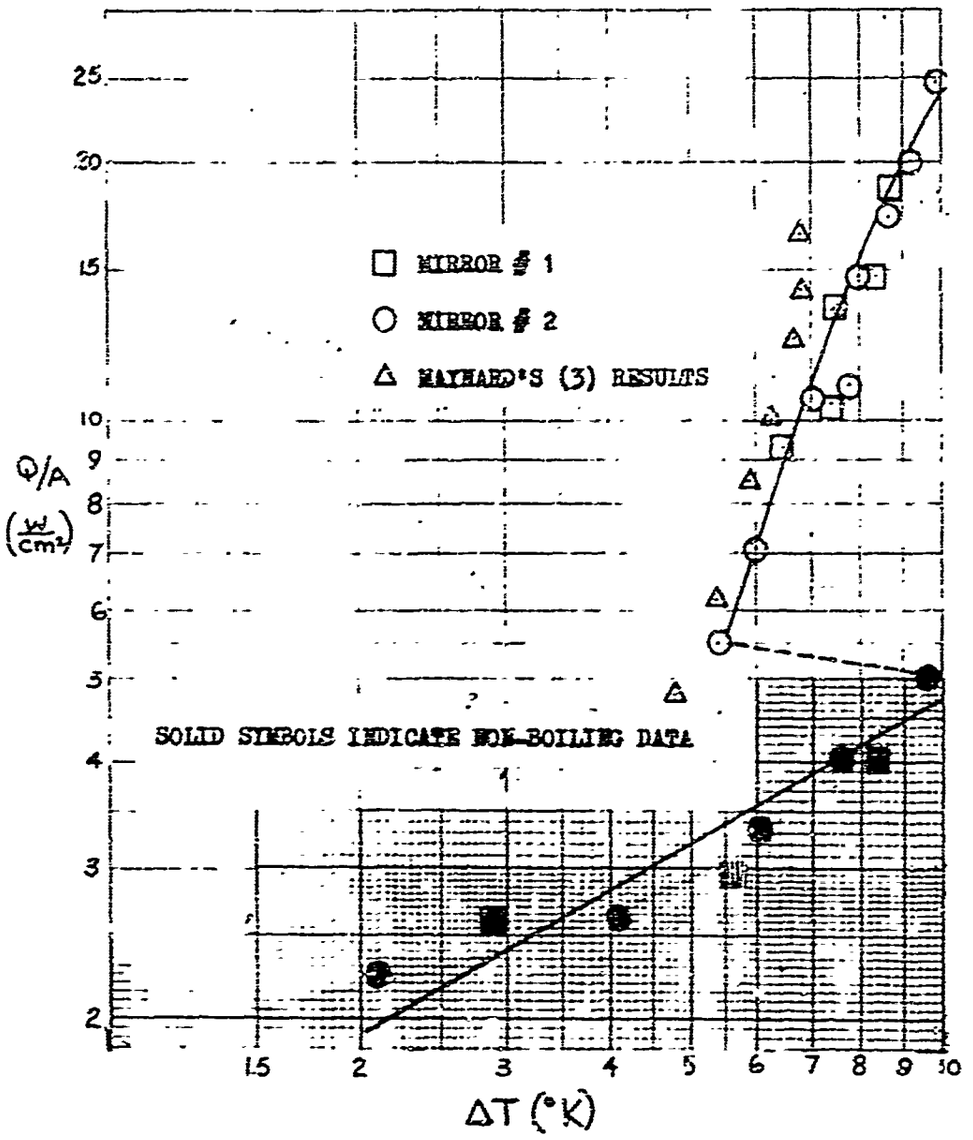

FIGURE 14 REPRODUCIBILITY OF NUCLEATE BOILING RESULTS SHOWING MAYHARD'S RESULTS (MIRROR COPPER SURFACE)

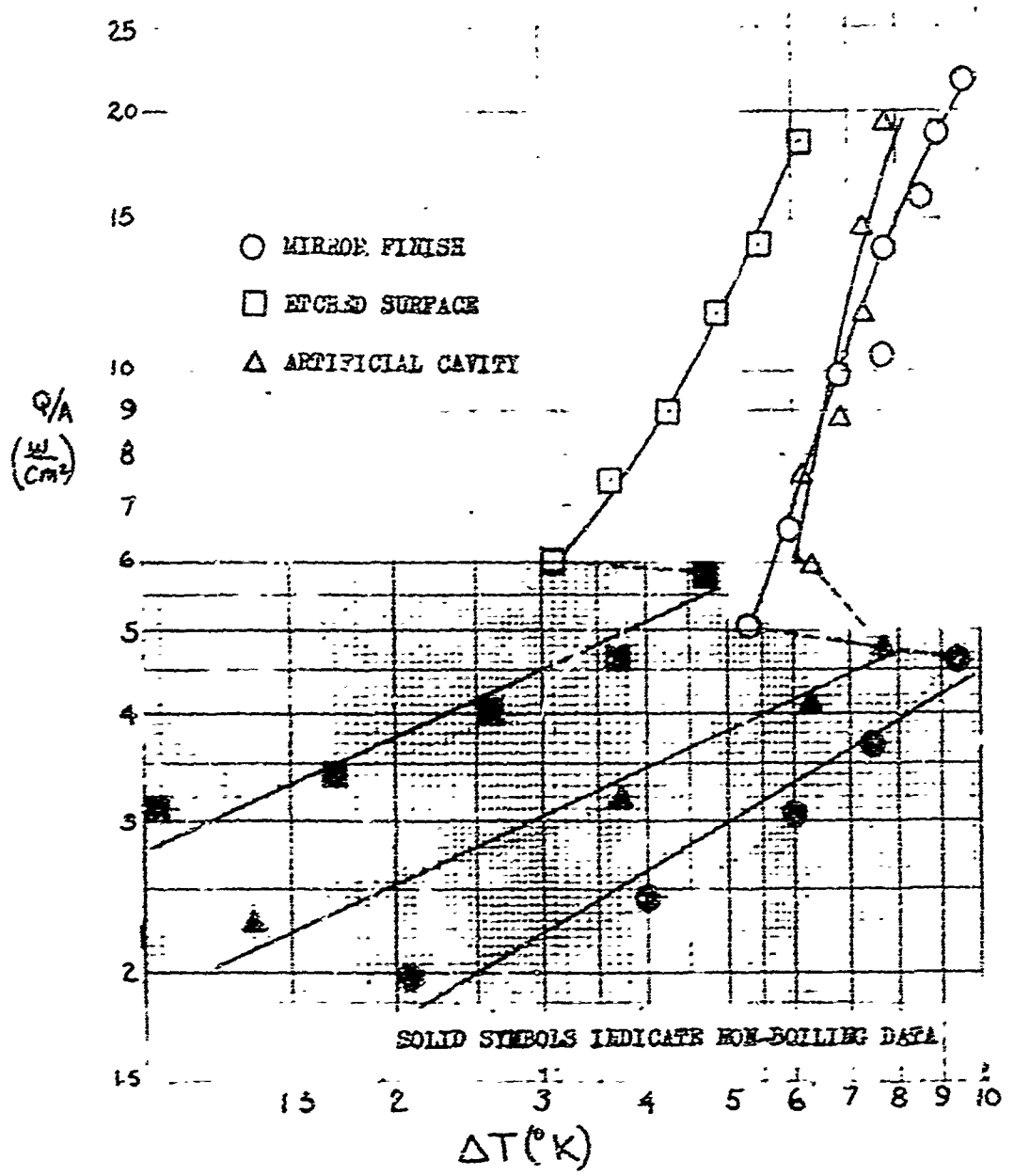

FIGURE 15 SUMMARY OF SURFACE EFFECTS ON NUCLEATE BOILING FOR COPPER

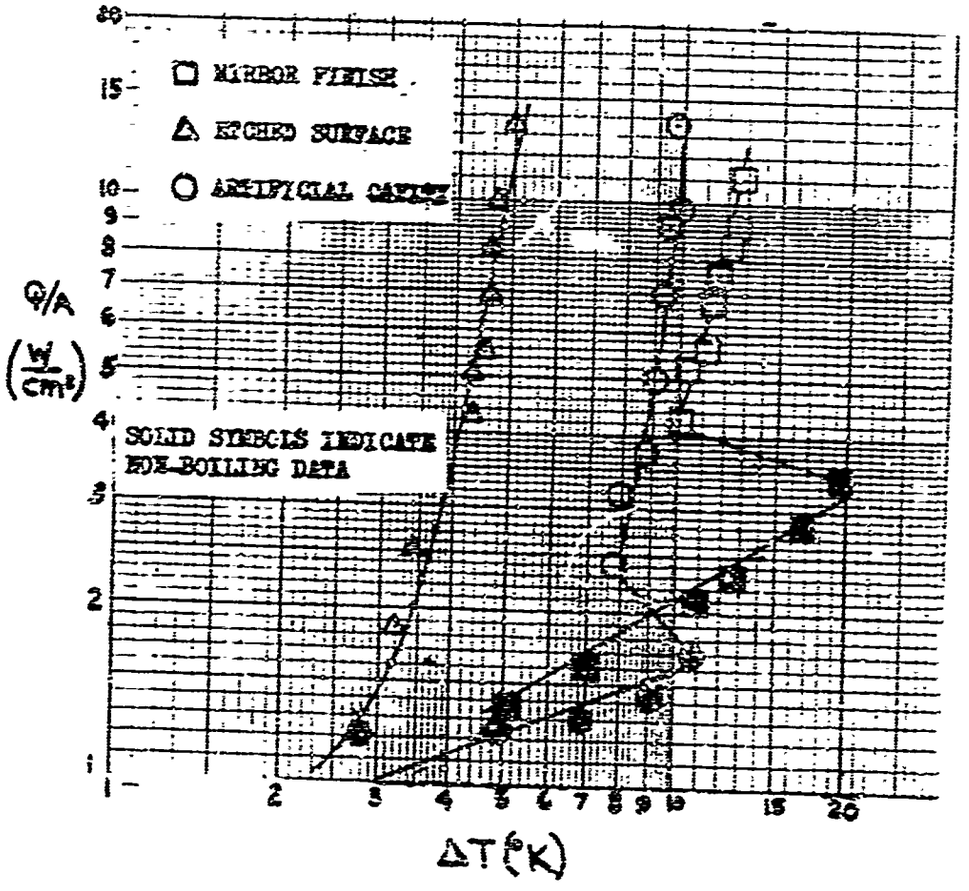

FIGURE 16 SUMMARY OF SURFACE EFFECTS ON NUCLEATE BOILING FOR NICKEL

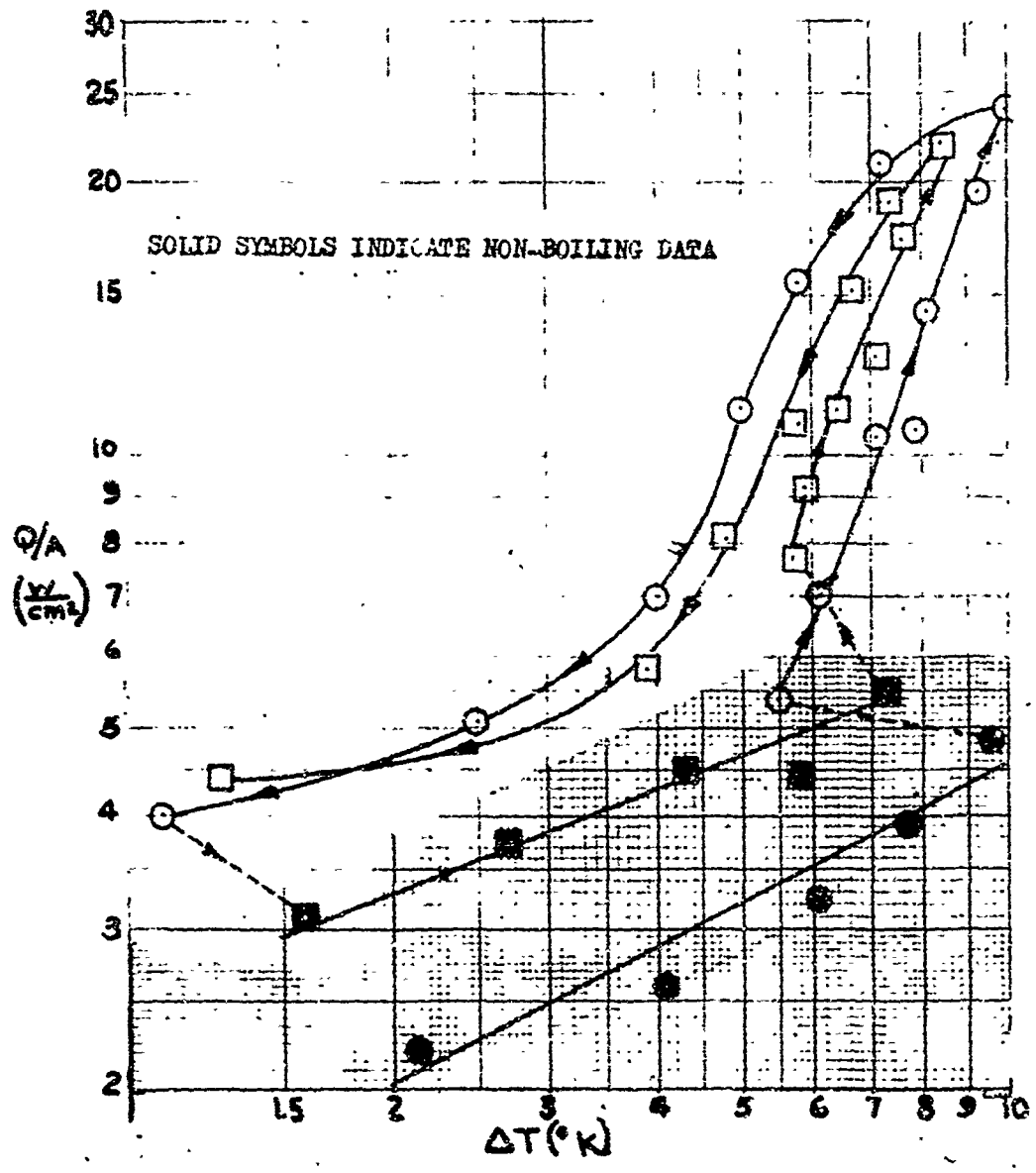

FIGURE 17 MIRROR FINISHED COPPER SURFACE SHOWING HYSTERESIS

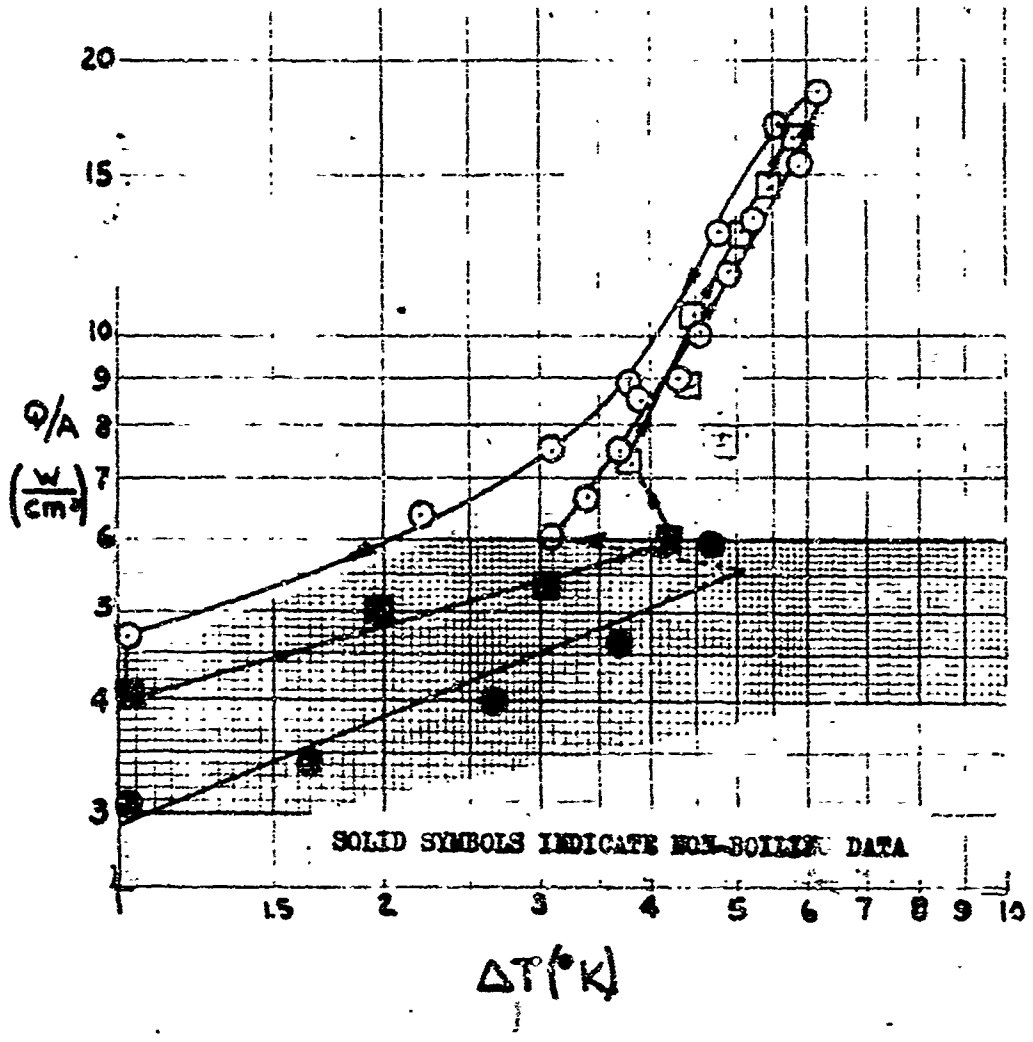

FIGURE 18 ETCHED COPPER SURFACE SHOWING HYSTERESIS

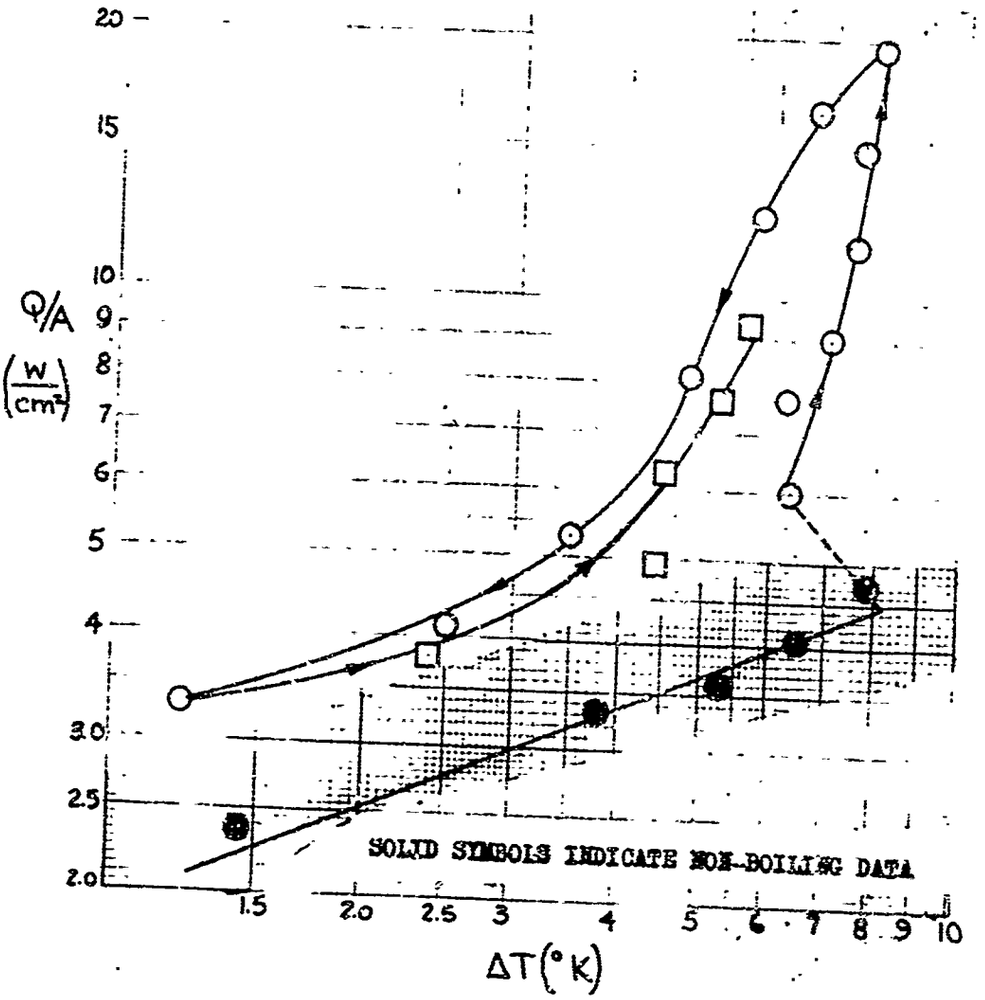

FIGURE 19 MIRROR FINISHED COPPER SURFACE WITH ARTIFICIAL CAVITY SHOWING HYSTERESIS

INITIAL DISTRIBUTION LIST

		No. Copies
1.	Defense Documentation Center Cameron Station Alexandria, Virginia 22314	20
2.	Library Naval Postgraduate School Monterey, California 93940	2
3.	Professor P. J. Marto Department of Mechanical Engineering Naval Postgraduate School Monterey, California 93940	2
4.	LT H. W. George, USN USS NORTHAMPTON (CC-1) FPO New York 09501	1

UNCLASSIFIED

Security Classification

DOCUMENT CONTROL DATA - R&D

(Security classification of title, body of abstract and indexing annotation must be entered when the overall report is classified)

1. ORIGINATING ACTIVITY (Corporate author)	2a. REPORT SECURITY CLASSIFICATION
Naval Postgraduate School Monterey, California 93940	Unclassified
	2b. GROUP

3. REPORT TITLE

AN EXPERIMENTAL INVESTIGATION OF SURFACE EFFECTS ON NUCLEATE POOL BOILING OF LIQUID NITROGEN FROM A HORIZONTAL SURFACE

4. DESCRIPTIVE NOTES (Type of report and inclusive dates)

Thesis

5. AUTHOR(S) (Last name, first name, initial)

GEORGE, Harold Wayne, Lieutenant, U. S. Navy

6. REPORT DATE	7a. TOTAL NO. OF PAGES	7b. NO. OF REFS
June 1967	73	17

8a. CONTRACT OR GRANT NO.	9a. ORIGINATOR'S REPORT NUMBER(S)
b. PROJECT NO.	
c.	9b. OTHER REPORT NO(S) (Any other numbers that may be assigned this report)
d.	

10. AVAILABILITY/LIMITATION NOTICES

This document is subject to special export controls and each transmittal to foreign nationals may be made only with prior approval of the Naval Postgraduate School.

11. SUPPLEMENTARY NOTES	12. SPONSORING MILITARY ACTIVITY

13. ABSTRACT

The effect of various surface conditions on the characteristic boiling curve for liquid nitrogen was experimentally investigated. A circular horizontal flat plate five square centimeters in area was utilized as a boiler surface.

The surfacesinvestigated included mirror finished surfaces, etched surfaces, and surfaces with .0043 inch diameter artificial cylindrical cavities. Each of these surface conditions was used with Electrical Tough Pitch Copper and Nickel 200 boiling surfaces.

The results indicate that surface conditions significantly affect the heat transfer coefficents during nucleate pool boiling of liquid nitrogen. Results from hysteresis data indicate that once boiling sites become active they tend to remain active and produce higher heat transfer rates.

DD FORM 1 JAN 64 1473

UNCLASSIFIED

Security Classification

14 KEY WORDS	LINK A		LINK B		LINK C	
	ROLE	WT	ROLE	WT	ROLE	WT
NUCLEATE BOILING						
HEAT TRANSFER						
CRYOGENIC						
LIQUID NITROGEN						